DGLR-2005-029NW

Mission Analysis of the Micro-Satellite *Flying Laptop*

M. Gauer, G. Grillmayer

Institute of Space Systems, University of Stuttgart
Pfaffenwaldring 31, 70550 Stuttgart, Germany
gauer@irs.uni-stuttgart.de

ABSTRACT

The *Flying Laptop* is a micro-satellite currently under development by the Institute of Space Systems (IRS). Due to the launch as a piggy-back payload the orbital parameters depend on the primary payload and launch opportunity. In order to verify the satellite's pointing modes in connection with the attitude sensors, specially the star tracker, an analysis is performed to show that the current star tracker baffle design is sufficient for the planned scientific measurements. The orbital parameters, eclipse times as well as the contact times to the IRS ground station are calculated and discussed.

Acronyms

ACS	Attitude Control System
BRDF	Bi-directional Reflectance Distribution Function
CHU	Camera Head Unit
FOV	Field Of View
IRS	“Institut für Raumfahrtsysteme”, Institute of Space Systems
ISRO	Indian Space and Research Organization
LTAN	Local Time of Ascending Node
LTDN	Local Time of Descending Node
PSLV	Polar Satellite Launch Vehicle
SSO	Sun-Synchronous Orbit
STK	Satellite Tool Kit

1. INTRODUCTION

Within the scope of the Stuttgart Small Satellite Program several satellites are being developed and built at the Institute of Space Systems. The *Flying Laptop* [1],[2] will initiate the program's operational commencement. Its mission objectives can be merged under two major subjects, technology demonstration in regard to the upcoming missions and scientific research in chosen areas.
To get a first glance into the course of specific mission scenarios [3], to optimize the arrangement of specific components whose performance depends mainly on environmental conditions, or to analyze effects on mission performance of orbital parameters or configuration changes, simulation software is of great help and importance for the success of the upcoming mission. The orbit analysis of the micro-satellite *Flying Laptop* is being conducted by using the simulation tool Satellite Tool Kit [4].
A variation of the orbital parameters changes the sunlight and umbra times, access times to the ground station, frequency of the scientific measurements, charging times and also the attitude sensor requirements which in turn leads to different designs of the satellite.
Additionally, the possibility of implementing 3D-models into STK offers the chance for students and employees of the IRS to understand and to reconstruct the process of specific scenarios much easier.

2. MISSION ANALYSIS

2.1. Orbit Properties

The *Flying Laptop* will be launched as a piggy-back payload, i.e. its orbit is dependent on the requirements of the primary payload. The

Indian PSLV rocket is intended to be used as the launch vehicle. Taking into account previous PSLV launches by ISRO and an Earth observation primary payload the orbit altitude can be assumed with high probability to be within 500 to 900 km and the LTDN between 09:30h and 11:00h. The orbit is sun-synchronous.

Eccentricity

Since the orbit will be close to circular the eccentricity *e* is assumed to be zero for the simulations.

Semi-major Axis

This threshold has to be considered in the simulations since different heights result in various sunlight, visibility and observation conditions. It also determines the repeat path and revisit times.
Lower orbits require higher slew rates of the attitude system control loops. An altitude of 600 km was chosen for the simulations of the ACS.

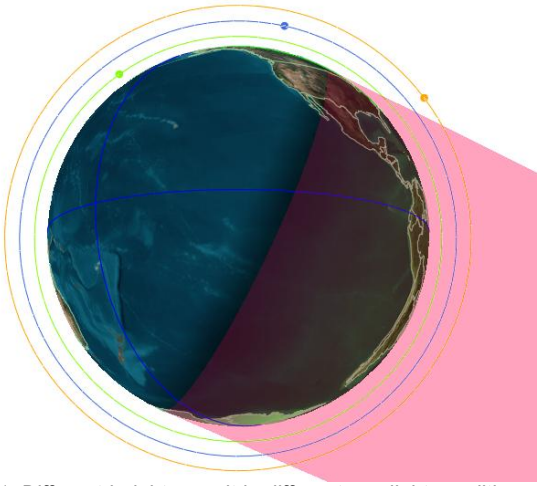

Figure 1: Different heights result in different sunlight conditions

Figure 1 shows different orbit heights. In a 500 km, 10:30h orbit the sunlight phase is approx. 63.8% while in a 900 km orbit it is 68% of the orbital period.

Inclination

For a sun-synchronous orbit the given three parameters *a*, *e* and *i* have the relationship of Eqn. (2.1). The Earth's oblateness causes a secular precision of the orbital plane of nearly 1 °/day at the nodal line in eastward direction.

$$\cos(i) = -\frac{2}{3}\sqrt{\frac{R_E^3}{\mu}}\frac{1}{J_2}\frac{2\pi}{T_{orbit}}\left(1-e^2\right)^2\left(\frac{a}{R_E}\right)^{\frac{7}{2}} \quad (2.1)$$

$$T_{orbit} = 2\pi\sqrt{\frac{a^3}{\mu_E}} \quad (2.2)$$

For a circular (*e* = 0) sun-synchronous orbit, having a constant secular motion and an orbital period as given in Eqn. (2.2), Eqn (2.1) results in

$$\dot{\Omega} = -\frac{3}{2}\sqrt{\frac{\mu_E}{a^3}}J_2\frac{R_E^2}{a^2}\cos(i)\,. \quad (2.3)$$

Thus the inclination *i* in [rad] can be calculated by Eqn (2.4) using $J_2 = 1.083\cdot10^{-3}$ and $\dot{\Omega} = 1.99106361\cdot10^{-7}\,rad/s$.

$$i = \arccos\left(\frac{\dot{\Omega}}{-\frac{3}{2}\sqrt{\frac{\mu_E}{a^3}}J_2\frac{R_E^2}{a^2}}\right) \quad (2.4)$$

For a sun-synchronous, circular orbit the inclination is a function solely of the altitude and corresponds to 97.79° for a 600 km orbit.

Longitude of Ascending Node

This parameter fully depends on the time of launch. This time coincides with the LTDN since the PSLV launches southward.
In Table 1 two orbits are defined for simulating the ACS in orbit. They differ only in LTAN. The range of LTAN has a higher impact on the attitude sensors than the altitude variation. Thus for all calculations below an altitude of 600 km in combination with the two boundary LTDN of 9:30h and 11:00h is used.

Orbit Parameter	Orbit 1 [SSO]	Orbit 2 [SSO]
Semimajor Axis	6978.137 km (h=600 km)	6978.137 km (h=600 km)
Inclination	97.79°	97.79°
Eccentricity	0	0
Local Time of Ascending Node LTAN	21:30:00 UTC	23:00:00 UTC

Table 1: Orbit parameters

2.2. Eclipse Times

The duration of the sunlight and umbra phase is very important for the determination of the power budget and the thermal control system. As the satellite can not be charged during the umbra phase the sizing of the battery depends among other things on the longest duration in which the satellite is not illuminated by the sun.
Due to the seasons the duration of the umbra

differs about 170 s between February and June. The penumbra phase connects the sunlight and the umbra phase with a mean duration of about 10 s. This short period of time can be neglected in these calculations.
The mean statistics for one year for both orbits are summarized in Table 2.

Phase	Duration [min] Orbit 1	Duration [min] Orbit 2
Sunlight - Mean	64.51	61.75
Umbra - Mean	31.88	34.72

Table 2: Statistics for Orbit 1 and Orbit 2

By comparing the duration of the different phases of both orbits it becomes apparent that the closer the launch is to local noon the longer the umbra phase takes.
Orbit 2 with its longer umbra and shorter sunlight phase is more critical for the battery and hence is used for the power simulations.

2.3. Ground Station Contact

The IRS with its own ground station will maintain the communication with the satellite. Due to vegetation and geometric perturbations an elevation angle of 7° needs to be taken into account. Figure 2 below shows the resulting communication boundaries for a 600 km orbit. A sample ground track is shown where the bold lines represent the area of access. The elevation angle of 7° is used for all the following simulation scenarios.

Figure 2: FOV for IRS with an elevation of 7°

The global statistics calculated for one calender year are illustrated in Table 3. For contacts with a duration of less than one minute the roll angle of the satellite nearly reaches its maximum as the ground station is situated significantly eastward or westward from the ground track. For use of the high gain antennas (requiring a pointing accuracy of 1°-2°) the satellite needs to be pointed toward the ground station in target pointing mode. Specifically at night, without a sun sensor, the feasibility of the maneuver depends solely on the star tracker and is discussed in section 3.

	Duration [min]
Access – Min Duration	0.35
Access – Max Duration	9.63
Access – Mean Duration	7.53

Table 3: Global statistics

The *Flying Laptop* will have a mean number of 4.83 contacts per solar day.
A property of the sun-synchronous orbit is that the orbit altitude may be chosen in a way to be in resonance with the Earth's rotation. After a certain number of days the ground track is repeated again. This number of days is called the orbit repeat cycle where the satellite will pass the ground station at the same times every cycle. A repeat cycle of 8 days or 119 orbits was calculated in our simulations.
Furthermore it is interesting to know when the satellite will enter the FOV of the ground segment for the first time after separation. The *Flying Laptop* will be launched from Sriharikota in India. After separation the satellite will fly without contact for nearly 3 orbits. The first access to the IRS ground segment takes place approximately 4.5 hours after launch. In the following orbit it will also be possible to access the satellite from the IRS ground station (Figure 2).

2.4. Orbital Drift

The main factors which cause orbital drift are the oblateness of the Earth and perturbations caused by the moon and sun's gravitational forces. A spacecraft launched to observe the target area at a specific local time will drift to later LTANs through its operational lifetime.
In order to get real-world values for drift estimation the Proba and DLR Tubsat micro-satellites, which are of equal size and mass to the *Flying Laptop,* were selected for comparison. They are not equipped with thrusters to perform active orbit control. For the two satellites TLEs were downloaded from SpaceTrack [5]. For Proba a drift rate ranging from 0.23°/year - 2.16°/year was determined. Though for DLR Tubsat drift rates of 3.2°/year and 4.7°/year for the first 2 years and 10.1°/year for the 5th year in orbit were found.
The mission design lifetime of the *Flying Laptop* is two years. To be on the safe side the

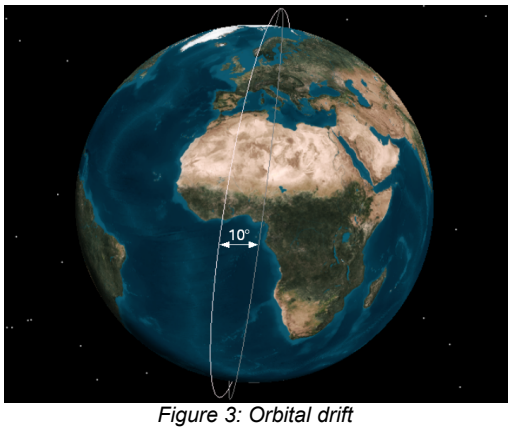

Figure 3: Orbital drift

drift angle can be estimated to be a maximum of 10° after this time (Figure 3).

2.5. Operational Scenarios

Different pointing modes of the *Flying Laptop* are used to obtain the orientation of the payload cameras necessary for optimal science outcome. The pointing modes are Inertial-Pointing, Nadir-Pointing and Target-Pointing.
In cases of a failure detection another mode has to be considered, the so called safe-hold mode which combines the detumbling and safe mode.

Nadir-Pointing Mode

In this mode, shown in Figure 4, the satellite is aligned in the direction of the Earth, i.e. the z-vector of the satellites body coordinate system points toward the Earth's center. The satellites rotates with a constant angular rate. This mode is also called the Earth-pointing mode, being used for image acquisition, attenuation measurements and trace gas detection.

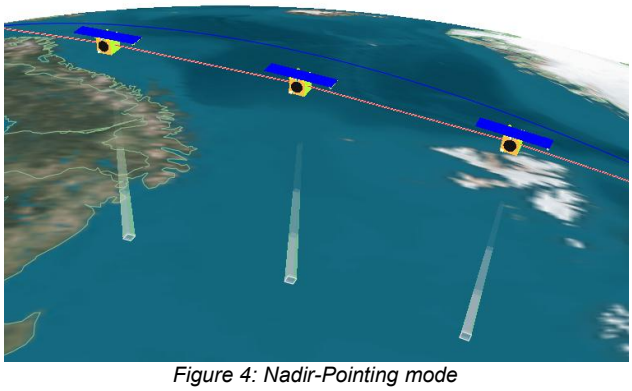
Figure 4: Nadir-Pointing mode

Inertial-Pointing Mode

With the satellite being aligned inertially (Figure 5) a pointing knowledge of 7 arcseconds can be realized with the help of the two star

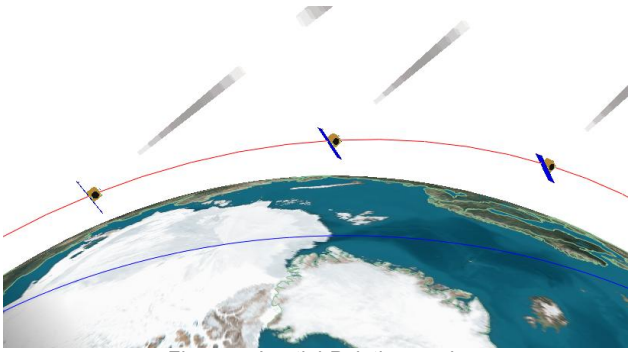
Figure 5: Inertial-Pointing mode

trackers. The satellite will be and will remain inertially stabilized as the name implies, i.e. the coordinate system of the satellite will maintain the same orientation in respect to the heliocentric inertial equatorial reference frame.
During charging of the battery the satellite's solar array is aligned to the sun, making also use of the inertial-pointing mode.

Target-Pointing Mode

In the target-pointing mode the satellite stays aligned to a fixed point on the Earth's surface. This mode is mainly used for scientific BRDF measurements, off-nadir inspection of ground areas and during contact with the IRS ground station using the high gain antennas. The BRDF-measurement needs to be conducted along ±60° pitch off nadir and with a maximum roll of ±5° (Figure 6).

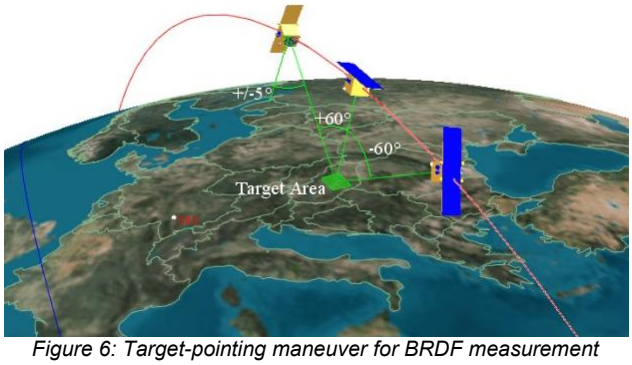

Figure 6: Target-pointing maneuver for BRDF measurement

Safe-Hold Mode

This mode performs the attitude recovery after a failure and the initial attitude acquisition after launcher separation. The Safe-Hold Mode performs rate reduction using simple equipment, only the magnetometers and the magnetic torquers are active. It is based on a simple magnetic control law known as the 'B-dot control law' [6]. The spacecraft will rotate twice per orbit around its pitch axis following the Earth magnetic field lines once the B-dot control law is converged. No sun sensor is

necessary in this mode as the spacecraft will be in a defined rotational state.
After the satellite rate is stabilized (2 rotations per orbit in orbital plane) and the battery is charged the satellite is ready to perform a mode transition.
It takes several orbits for the decrease of the initial rate due to the small magnetic moment of the magnetic torquers. While the spacecraft is tumbling after separation it is advantageous not to deploy the solar panels immediately due to a more continuous exposure of the solar cells with sunlight. After stabilization and communication with the ground station the panel deployment can be initiated.

3. STAR TRACKER ANALYSIS

3.1. Configuration and Constraints

The star tracker is the attitude sensor with the highest accuracy. It determines the pointing knowledge of images taken by the payload cameras. For images and BRDF measurements a pointing knowledge of 7 arcseconds is required.
The star tracker consists of the data processing unit and two camera head units. The location of the two CHUs and their baffles is illustrated in Figure 7 below. The x-axis points to the flight direction in nadir-pointing mode. Both CHUs are placed on the side of the satellite that is not lighted by the sun during nadir- and BRDF target-pointing. The field of view of both star trackers is shown in Figure 8. The two CHUs are elevated by 125° measured from the z-axis and are spread by 45°. The optical axes/boresight of the 13°x18° rectangular field of view of CHU A and CHU B is the reference from where all angles are measured.

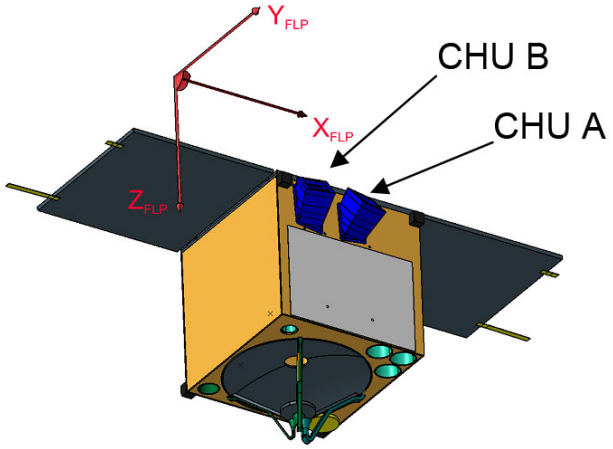

Figure 7: Location of the two Star Tracker Camera Head Units

The accuracy of the star tracker depends on environmental conditions, especially the direction of the sunlight and the albedo radiation of the Earth relative to boresight of the camera head units. To avoid blinding due to the sun the angle from the optical axis to the sun must be higher than 55°. On the other hand the angle to the Earth's limb (here defined as the beginning of the mesopause at 80 km above the Earth surface) must not be less than 25°. Both values depend on the length and shape of the star tracker baffles and will be known exactly after the baffles are built.

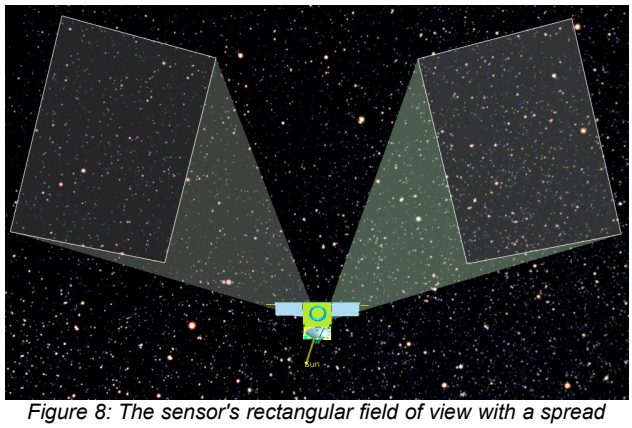

Figure 8: The sensor's rectangular field of view with a spread angle of 45°

The minimum angle between the CHUs and the sun decreases with the nodal passage approaching local noon (12:00h) while the angle from the CHUs to the Earth limb is independent of the nodal passage. Hence, Orbit 2 defines the worst case and is therefore used for all simulations of the star tracker.
For all pointing maneuvers where high pointing knowledge is required the angle between the star tracker and the sun as well as the angle between the star tracker and the Earth need to be examined. Maneuvers must be avoided where an attitude solution cannot be obtained from the star trackers due to blinding.

3.2. Nadir-Pointing

During nadir-pointing the angles from both CHUs to the earth limb are constantly at 57.7°. The minimum angle to the sun is 60.5° for CHU A and 57.5° for CHU B. The minimum angle to the sun does not occur at the same time for both CHUs. Note the asymmetry due to an orbit inclination unequal to 90°.
Blinding due to the full moon occurs every month. Because the CHUs are 45° apart only one is blinded at a time while the other one can maintain a navigation solution.

3.3. Target-Pointing for BRDF

The pointing knowledge is specially important for BRDF measurements where the pitch angle range is ±60° off nadir and roll angle range is ±5° off nadir as mentioned earlier.
Three target areas were chosen for the simulated BRDF-measurements. They are situated on the sun facing side of the Earth and were chosen in a way to examine the maneuvers in high positive and negative latitudes and in the subsolar region. The target areas are assigned with the numbers in Table 4. In order to examine the feasibility of the maneuvers in the simulations all BRDF areas are observed during one orbit in a consecutive manner.

BRDF target	Location
1	Target area near Finland
2	Subsolar target area
3	Area southwards from sub-solar point

Table 4: BRDF target areas

Angle between both CHUs and sun during BRDF measurements

The plots in Figure 9 illustrate the variations of the angle between boresight and the sun during the BRDF maneuvers. Numerical values from Figure 9 are shown in Table 5. The critical angle of 55° is almost reached by CHU A and CHU B at target 2 and slightly under-run for CHU B at target 3.

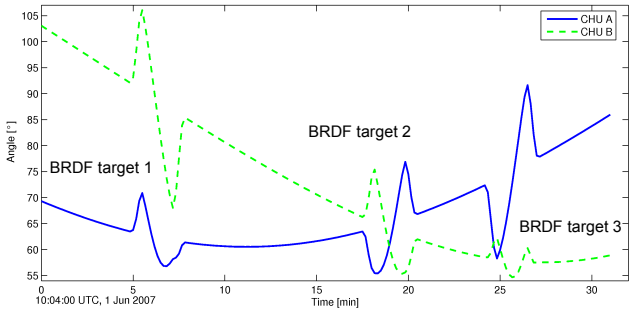

Figure 9: Angle between the boresight of CHU A, B and the sun

BRDF target	UTC [hh:mm:ss]	CHU A min. angle [°]	CHU B min. angle [°]
1	10:10:50	56.8°	
1	10:11:10		68.0°
2	10:22:20	55.4°	
2	10:23:30		55.6°
3	10:28:50	58.3°	
3	10:29:40		54.7°

Table 5: Minimum angles for CHU A and CHU B during BRDF maneuvers.

Nevertheless the other CHU has in any case at the same time a higher angle than 55°. Hence the chart and numbers show that even during worst case conditions, i.e. when the target area is located exactly subsolar, the star tracker system can obtain a precise navigation solution.
A polar plot, which is another representation of the same BDRF scenario is shown in Figure 10. From a sensor point of view the sun moves

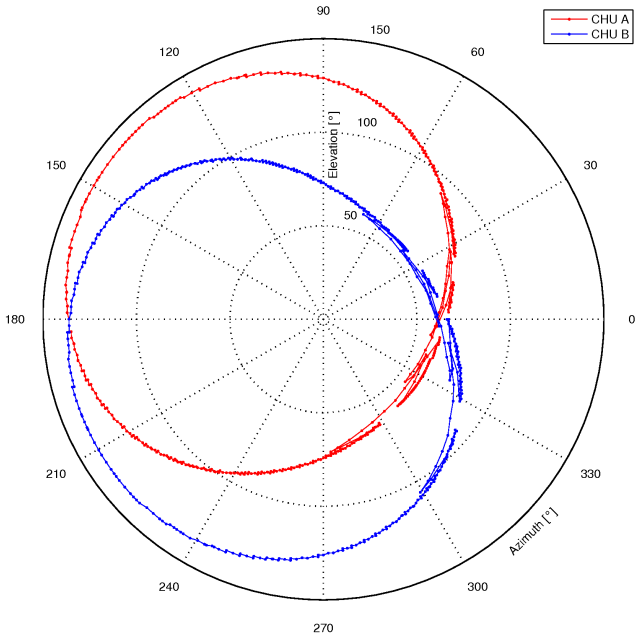

Figure 10: Polar plot of the BRDF maneuvers during one orbit

around the optical axis of the sensor. The boresight of each CHUs is located in the center of the diagram with the elevation angle plotted in radial direction while the azimuth angle to the sun forms the outer circle. The time step between two points is 10 s and a full orbit is shown.

Angle between both CHUs and Earth limb during BRDF measurements

The maximum roll angle of 5° remains constant during the simulation of the three BRDF maneuvers. The graph in Figure 11 shows the angle between the CHUs and the Earth limb. The minimum angle for both CHUs to the Earth's limb during target-pointing is equal to 40.4°. Therefore enough margin to the critical value of 25° is available at any time.
In combination with the results of the sun exclusion angles above it can be seen that BRDF measurements are always realizable with high precision because the critical angle for blinding of the star tracker system through the sun and Earth albedo is never reached or

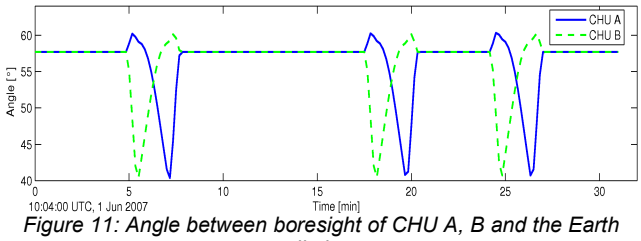

Figure 11: Angle between boresight of CHU A, B and the Earth limb

transgressed by both CHUs at the same time.

3.4. Target-pointing for ground station access

For target-pointing maneuvers where the high gain antennas of the *Flying Laptop* are used for communication with the IRS ground station, other limits than for the BRDF measurements apply. The roll angle during the maneuvers is much higher when the ground station is located far east- or westward of the ground track. This denotes that the angle from the CHUs to the sun could clearly fall below the critical value of 55° when the satellite points westward or the angle from the CHUs to the Earth limb could fall below the threshold of 25° when pointing far eastward.
Figure 12 illustrates an example where the angle between one CHU and the sun is 14°. The value for the other CHU is similar and thus the star tracker cannot provide an attitude solution.
Because the antennas only require a relatively relaxed pointing accuracy in the 1° range, the sun sensors, which have a 4π field of view, can be utilized to support the maneuver.

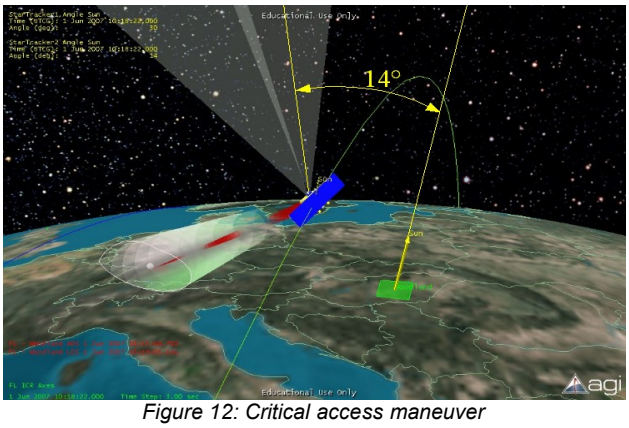

Figure 12: Critical access maneuver

As a consequence it can be generalized that ground station access using the target pointing mode is possible during the day but relies on the sun sensors in addition to the star tracker and GPS. Ground communications while the satellite is at the night side are limited by a maximum roll angle to the West.

4. CONCLUSIONS

With the aid of STK the orbital parameters of the micro-satellite *Flying Laptop* as well as the operational modes with regard to the observation of target areas could be determined and simulated. Evaluation of the orbit parameters by using data of previous satellites launched with the intended PSLV launcher were performed. Two orbits were selected for the simulations. The orbital drift, eclipse times as well as the contact times to the IRS ground station were calculated and discussed.
It is shown that the precision BRDF measurements are possible using the current star tracker design. Furthermore it can be seen that target-pointing in order to communicate with the ground station relies on the sun sensor and cannot always be carried out.

5. REFERENCES

[1] G. Grillmayer, A. Falke, H.-P. Roeser, *Technology Demonstration with the Micro-Satellite Flying Laptop*, Selected proceedings of the 5th IAA Symposium on Small Satellites for Earth Observation, IAA-B5-1402, p.419-427, Berlin, Germany, April 4-8, 2005.

[2] H.-P. Roeser, M. v. Schoenermark, F. Huber, G. Grillmayer, M. Lengowski, S. Walz, A. Falke, T. Wegmann, *Earth Observation with the Small Satellite Flying Laptop of the University of Stuttgart*, 9th ISU Annual International Symposium, Strasbourg, France, Nov. 30 – Dec. 3, 2004.

[3] M. Gauer, *Missionsanalyse und Orbit-simulation des Kleinsatelliten Flying Laptop,* Student Research Project, IRS-05-S-19, Institut für Raumfahrtsysteme, Stuttgart, 2005.

[4] AGI, Analytical Graphics, Inc, *Satellite Tool Kit*, STK Version 6.1.3, 2004.

[5] U.S. Government, *SpaceTrack – The Source for Space Surveillance Data*, http://www.space-track.org

[6] Y.W. Jan, J.C. Chiou, *Attitude control system for ROCSAT-3 microsatellite: a conceptual design*, Acta Astronautica 56, p.439-452, 2005.